

Article

Density Functional Theory Study of CO Hydrogenation on a MoS Surface

Min Huang, and Kyeongjae Cho

J. Phys. Chem. C, **2009**, 113 (13), 5238-5243 • DOI: 10.1021/jp807705y • Publication Date (Web): 06 March 2009

Downloaded from <http://pubs.acs.org> on May 6, 2009

More About This Article

Additional resources and features associated with this article are available within the HTML version:

- Supporting Information
- Access to high resolution figures
- Links to articles and content related to this article
- Copyright permission to reproduce figures and/or text from this article

[View the Full Text HTML](#)

Density Functional Theory Study of CO Hydrogenation on a MoS₂ Surface

Min Huang and Kyeongjae Cho*

Department of Materials Science and Engineering and Department of Physics, The University of Texas at Dallas, Richardson, Texas 75080

Received: August 29, 2008; Revised Manuscript Received: December 12, 2008

CO hydrogenation on a MoS₂ surface has been investigated by means of the density functional theory method. CO was found to adsorb on the bridge position of the Mo-edge of a MoS₂ surface with a tilted configuration. However, this tilted configuration is unlikely to dissociate into O and C on the MoS₂ surface, which is different from CO adsorbed on a pure Mo metal surface. These differences are explained by their different structural properties and the different catalyst activities of the surfaces themselves, indicated by different electronic properties below the Fermi level. The reaction route analysis reveals methane and CO₂ as the main products of the CO hydrogenation reaction on a pure MoS₂ surface, which agrees with the experimental results.

I. Introduction

The Fischer–Tropsch process is an important industrial process. It offers potential to produce high-value transportation fuels or petrochemicals from biomass feedstock. The process begins with the production of syngas (either by gasification of coal and biomass sources or by re-forming natural gas), which is then reacted over a suitable catalyst to yield a wide range of products, containing mainly *n*-alkanes and *n*-alkenes, ranging from methane and ethane to high molecular weight waxes, as well as oxygenates, including alcohols.

Transition-metal sulfide-based hydrotreating catalysts, specifically molybdenum sulfides, were developed in the early twentieth century^{1,2} and soon became extensively used in CO hydrogenation and hydrodesulfurization processes for the production of cleaner fuels.³ Their tolerance for sulfur represented a great advantage over noble metal catalysts, which are easily poisoned by even small amounts of sulfur. An early experimental study on effects of various potassium promoters on activity and selectivity of CO–H₂ reactions showed that MoS₂ itself yielded almost exclusively C₁–C₅ hydrocarbons composed mostly of linear alkanes.⁴ Similarly, thermodynamics analysis showed that without promoters, there is no alcohol formed on a MgO–SiO₂-supported MoS₂ catalyst; the only product is hydrocarbon, in which methane is the dominant species.⁵ A more recent in situ diffuse reflectance infrared Fourier transform (DRIFT) study on sulfide Mo/γ-Al₂O₃ catalysts showed that the main products of CO hydrogenation are CO₂ and CH₄.⁶ Murchison et al.⁷ of Dow Chemical Corporation discovered in the 1980s that alkali doping of MoS₂ would shift the selectivity of CO hydrogenation production from hydrocarbons to alcohols on undoped MoS₂. Further addition of promoters on an alkali-doped MoS₂ surface such as Ni or Co would increase the selectivity of the reaction toward ethanol and higher alcohols.^{8–12} These reactions are complicated as they may involve many complex elementary reaction steps such as dissociative and nondissociative adsorption of H₂ and CO, C–C bond formation, C–H bond formation, O–H bond formation, and CO insertion into the surface alkyls on a MoS₂ surface. The reaction mechanisms are very likely to be diverse, and it

is generally assumed that the reaction proceeds via a number of parallel reaction pathways.¹³

The most typical heterogeneous catalyst used in the Fischer–Tropsch synthesis is Fe/Ru/Co supported on an oxide such as silica, often promoted with potassium and other additives. Surface studies have shown that a CO molecule dissociates spontaneously on an iron surface.^{14–16} On the other hand, both experimental and theoretical studies have shown that CO adsorbs molecularly on a Mo surface with a tilted configuration; however, it dissociates easily into atomic carbon and oxygen.^{17–21} It is calculated that the activation energy for CO dissociation on a Mo surface ranges from 0.45 to 0.56 eV, resulting in lower energies of 1.71 and 0.59 eV after dissociation at the CO coverage of 0.25 and 0.5 ML, respectively.²¹ However, CO adsorption on a MoS₂ surface behaves differently from Mo metal, as only molecularly adsorbed CO species were reported by X-ray photoelectron spectroscopy (XPS)²² and IR studies.^{23–25} A recent DFT calculation²⁶ on CO adsorbed on stoichiometric and nonstoichiometric molybdenum sulfide surfaces showed CO tightly adsorbed on the MoS₂ surface with adsorption energy as high as 1.94 eV. Meanwhile, most transition metal surfaces are known to dissociate H₂ into atomic hydrogen. Previous studies also showed that H₂ molecules spontaneously dissociate on a MoS₂ surface.^{27,28} Hence, CO hydrogenation reaction mechanics and reaction pathways on a MoS₂ surface are predicted to likely be very different from those on metal surfaces. To our knowledge, although the interactions of CO and H₂ on MoS₂ were well-studied^{22–28} and much experimental research on hydrogenation reactions from syngas on MoS₂ surfaces has been done,^{4–12} there are very few systematic theoretical studies on this topic. Identifying key mechanisms in controlling CO hydrogenation reactions leading to CH₄, CH₃OH, C₂H₅OH, and higher alcohols and hydrocarbons theoretically would be useful for improving the activity of catalysts by means of modifying catalysts or finding new potential catalysts in experiments. In this study, we performed a systematic density functional theory (DFT) study on the CO hydrogenation reaction on a pure MoS₂ surface and determined the relative energies of different reaction routes as well as the most favorable products.

* To whom correspondence should be addressed. E-mail: kjcho@utdallas.edu.

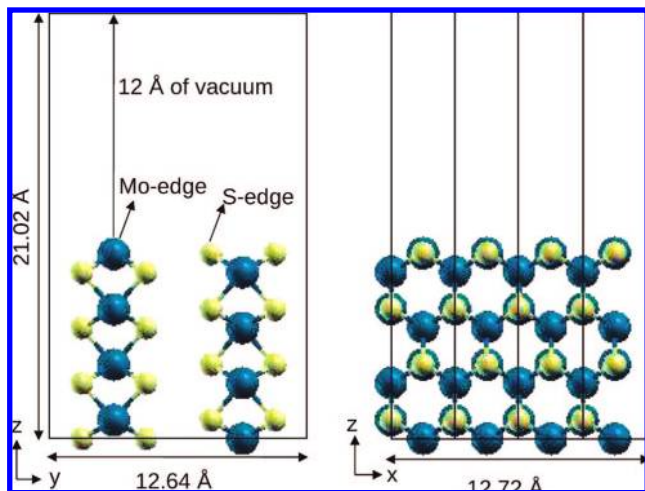


Figure 1. Edge surface of MoS₂ and the 4 × 1 supercell used in the calculation. Blue and yellow spheres represent Mo and S atoms, respectively.

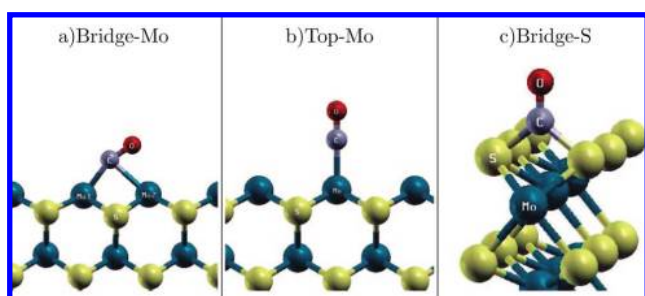


Figure 2. Optimized adsorption structures for CO adsorbed on a MoS₂ surface: (a) bridge-Mo, (b) top-Mo, (c) bridge-S. Blue, yellow, gray, and red spheres represent Mo, S, C, and O atoms, respectively.

II. Computational Method

Calculations were performed by using the Quantum ESPRESSO/PWscf computer package²⁹ and the generalized gradient corrected PW91 approximation³⁰ for the exchange and correlation functional. Electron-ion interactions were described by ultrasoft pseudopotentials,³¹ while wave function and electron density representation were described with a plane wave basis set and were limited by kinetic energies of 30 and 300 Ry, respectively. The *k*-point meshes employed in the calculations were generated according to the Monkhorst–Pack scheme.³² The resulting Brillouin zone sampling used for the supercells described below was equivalent to the one obtained with (8 × 8 × 1) grids for the primitive (1 × 1) cells of the surface. Energy barriers and transition states for reactions were calculated with the nudged elastic band (NEB) method.³³ Zero-point energy corrections were applied to the activation energy barriers. Vibration frequencies of the adsorbates were calculated using the frozen phonon method.

Bulk MoS₂ is a hexagonal structure with six atoms per unit cell, consisting of a single layer of S–Mo–S. The basal plane (001) is fully covered by sulfur atoms and is inactive for catalytic reactions. Cleavage of bulk MoS₂ parallel to the (100) or (010) plane results in an edge surface with a coordinatively unsaturated Mo-terminated edge (named Mo-edge or 10 $\bar{1}$ 0 edge plane) or alternately a S-terminated edge (named S-edge or $\bar{1}$ 010 edge plane) (Figure 1). The same edge surfaces were found in the experimentally triangular-shaped, single-layer MoS₂ nanoparticles grown on a reconstructed Au (111) surface.^{34,35} Our calculation result also indicates the (100) edge surface being

the most stable with the lowest surface energy except for the basal (001) plane which is inactive; hence, only the edge surface will be considered in this study.

The (100) edge surface was modeled with tetragonal (4 × 1) supercell slabs consisting of eight atomic layers. We used our theoretical equilibrium lattice parameters of *a* = *b* = 3.18 Å and *c* = 12.6 Å and a vacuum thickness of 12.0 Å to build the supercell shown in Figure 1. The vacuum gap was tested to give good convergence. The CO and H₂ molecules and reactants were adsorbed on one side of the supercell; the coordinates of the atoms in the upper four layers of the slab (containing the adsorbates) were relaxed, while the rest of the atoms in the lower half of the slab were fixed at their bulk positions. The atoms were relaxed according to the Hellmann–Feynman forces until the force on each atom was less than 0.02 eV/Å. We compared the calculated results of CO, H₂, atomic C and O, and H adsorption on (100) full surface (with both Mo-edge and S-edge, the system size is double of that of Mo-edge only) and on Mo-edge or S-edge only. The most stable configurations are consistently located on Mo-edge, and the adsorption energy difference is less than 0.10 eV, which is considered to be within the computational error bar because the lowest adsorption energy is 1.41 eV for H₂ on MoS₂. Because the Mo-edge and S-edge have distinct chemical behaviors, the reactions on the two edges will be considered independently following previous studies.²⁷

III. Results

In CO hydrogenation reactions with syngas, CO molecules first adsorb on MoS₂ surfaces and then participate in elementary reaction steps, including dissociation and reacting with hydrogen to yield products. Therefore, identification of the energetic, structural, and electronic properties of CO and H₂ adsorbed on a MoS₂ surface could increase our understanding of CO hydrogenation on MoS₂ catalysts and facilitate the search for more effective catalysts.

A. CO Adsorption and Dissociation on a MoS₂ Surface.

CO molecules were found to chemisorb on the Mo-edge and S-edge of MoS₂ surfaces with adsorption energy ranging from 0.79 to 2.24 eV. The C–O bond length elongates from the calculated value of 1.14 Å for free CO (1.13 Å for experiment³⁶) to 1.22 Å (Table 1). Optimized adsorption configurations are shown in Figure 2. Our calculated adsorption energies are slightly larger than those from the previous DFT study,²⁶ and the CO vibration frequencies and C–O bond lengths are in good agreement. Furthermore, the calculated CO vibration frequencies are in reasonable agreement with the IR spectra of adsorbed CO on unsupported MoS_x, which shows a broadband at 2070 cm⁻¹ with a tail extent to 2000 cm⁻¹.^{22–24} The bridge-Mo (B-Mo) CO at the Mo-edge (Figure 2a) is a tilted configuration, and it is expected to be more activated than the end-on top-Mo configuration (Figure 2b) because of its longer C–O bond length and lower vibration frequency. We can estimate that the barrier energy for the adsorbed molecular CO diffusion on the MoS₂ surface is likely to be around 0.2 eV. Adsorbed molecular CO was predicted to easily diffuse from the B-Mo site to the symmetrically equivalent site because of the small energy difference between CO at the bridge site and at the top site (top site structure is the transition state).

The dissociation of CO might be one of the key steps of the CO hydrogenation reaction. Atomic C was found to adsorb on a Mo-edge of a MoS₂ surface at a bridge-Mo site with a binding energy of 10.31 eV (Table 2). An asymmetric configuration at a bridge-Mo site was identified with an energy slightly higher by 0.11 eV than that of the bridge configuration. The most stable

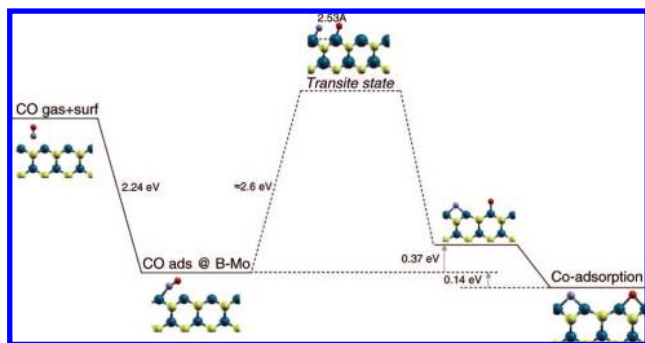
TABLE 1: Calculated Adsorption Energies, E_{ads} , C–O Bond Lengths, $L_{\text{C-O}}$, and CO Vibration Frequencies, ν , for the Stable and Metal Stable Adsorption Modes of CO on a MoS₂ Edge Surface and Mo Metal Surface

adsorption mode	E_{ads} (eV)	$L_{\text{C-O}}$ (Å)	ν (cm ⁻¹)
bridge-Mo (Mo-edge)	2.24, 1.93 ²⁶	1.223, 1.229 ²⁶	1551, 1545 ²⁶
top-Mo (Mo-edge)	2.05, 1.94 ²⁶	1.169, 1.154 ²⁶	1942, 1970 ²⁶
bridge-S (S-edge)	0.79, 0.51 ²⁶	1.198, 1.194 ²⁶	1725, 1781 ²⁶
H–Mo (Mo surface)	3.17, 3.08 ²¹	1.335, 1.387 ²¹	839, 969 ²¹

TABLE 2: Calculated Adsorption Energies of C, O, H, OH, CH_x, and CO₂ on a MoS₂ Surface^a

adsorbates	adsorption mode	adsorption energy (eV)
C	bridge-Mo	10.31
O	bridge-Mo	7.27
H	bridge-Mo	3.05
OH	bridge-Mo	4.32
CH	bridge-Mo	6.48
CH ₂	bridge-Mo	4.55
CH ₃	tilted top-Mo	2.62
CH ₄	top-Mo	0.16
CO ₂	bridge-Mo	1.60

^a Adsorption energies are respective to the species in a vacuum.

**Figure 3.** Energy diagram for CO dissociation on a MoS₂ surface.

configuration of atomic O adsorbed on a Mo-edge of a MoS₂ surface is the bridge-Mo site with a binding energy of 7.27 eV. The metastable configuration is at a top-Mo site, which is 0.6 eV higher in energy than the one at the bridge site. The coadsorption of atomic C and O results in the most stable configuration with C and O located at the B-Mo sites. The next stable configuration is with atomic C at a B-Mo site and O located at a top-Mo site. The calculated energy difference between the two configurations is 0.51 eV. Figure 3 shows the energy diagram of CO dissociated on a Mo-edge of a MoS₂ surface. Although the dissociated configuration is 0.14 eV more stable than that of CO adsorbed at B-Mo site, the barrier energy was predicted to be 2.60 eV, which is higher than the adsorption energy (2.24 eV). The adsorbed CO molecule desorbs rather than dissociates on a MoS₂ surface. The calculated barrier energy for CO dissociation on a Mo metal surface is 0.74 eV, which is slightly larger than the value of 0.58 eV in the previous study.²¹ Hence, dissociation of CO is fairly difficult on a Mo-edge of a MoS₂ surface, which is significantly different from a Mo metal surface. In the configuration of the transition state, the C–O distance is 2.53 Å, which is 1.31 Å longer than that of the CO adsorbed at the bridge, showing the breaking of the C–O bond. Dissociated C and O are located at the tilted top-Mo site, which is a metastable site for adsorption of O and C. The frequency calculation showed an imaginary frequency obtained, confirming a transition state.

To understand the difference between the interactions of CO with a MoS₂ surface and Mo metal surface, we also studied the adsorption of CO on a clean Mo (100) metal surface. In

agreement with both experimental¹⁸ and previous theoretical studies,^{20,21} CO was predicted to adsorb in a tilted configuration at the 4-fold hollow sites on a Mo (100) surface, with a calculated adsorption energy of 3.17 eV and tilt angle of 56.5° with respect to the normal of the surface. The bond length of a CO molecule is elongated up to 1.35 Å, which is larger than in the case of a MoS₂ surface by 0.13 Å, resulting in CO being more reactive and easily dissociated, as shown by the low stretching frequency in Table 1. In the case of a MoS₂ surface, a C atom in adsorbed CO forms covalent bonds with two surface Mo atoms (Mo₁ and Mo₂) (Figure 2a) and an O atom. These bonding characteristics are indicated by the projected density of states (PDOS) of the C, O, Mo₁, and Mo₂ atoms in Figure 4a and the bonding charge density in Figure 4b. Bonding charge density was defined as the charge density difference between a system of CO adsorbed at the bridge-Mo of a MoS₂ surface and pure MoS₂ surface and free CO. The bonding charge densities shown in Figure 4b clearly reveal the charge redistribution due to CO adsorption mainly involves a CO molecule and two neighboring Mo surface atoms, showing the bond formed between a C atom and two Mo surface atoms. The C–O bond was predicted to be a double bond saturating the coordinates of a C atom. In the most stable 4-fold hollow structure of CO adsorbed on a Mo metal surface, a C atom binds with four Mo surface atoms allowing the C–O bond to break easily. The electronic properties of Mo atoms at a pure MoS₂ surface and Mo surface were compared in Figure 4c. The contributions of the d orbitals of surface Mo atoms on two surfaces are different at the Fermi level. The surface Mo atoms on a Mo metal surface showed high density of states below the Fermi level, indicating higher activities than those on a MoS₂ surface, which was confirmed by the higher adsorption energy of CO on a Mo metal surface.

On the other hand, CO was found to adsorb at a S-edge of a MoS₂ surface at a B-S site (Figure 2c) with an adsorption energy of 0.79 eV, which is much weaker than in the case of a Mo-edge. The barrier energy of CO dissociation is predicted to be as high as 5.0 eV, which is larger than the calculated barrier energy for the diffusion of adsorbed CO from S-edge to Mo-edge (2.30 eV). Adsorbed CO molecules would prefer to diffuse to the Mo-edge rather than dissociate. Therefore, only the calculations on a Mo-edge of a MoS₂ surface will be considered.

B. H₂ Molecule and Atomic H Adsorbed on a Mo-Edge of a MoS₂ Surface. A H₂ molecule spontaneously dissociates on a Mo-edge of a MoS₂ surface forming a H–Mo bond. The calculated dissociative adsorption energy is 1.41 eV, with respect to a H₂ molecule in a vacuum, which is smaller than the calculated dissociative adsorption energy (1.68 eV) of H₂ on a Mo (100) surface. However, it is larger than the calculated value of 0.92 eV for a Mo metal surface,³⁷ for which the calculations were done on a bcc (210) surface rather than the flat (100) surface we used. Dissociation of a H₂ molecule was also predicted in a fully and partially sulfide Mo-edge.²⁷ Atomic H adsorbed at a bridge-Mo site was found to be most stable, and a metastable structure at a top-Mo site was identified to be 0.20 eV less stable than the most stable one. We found that atomic

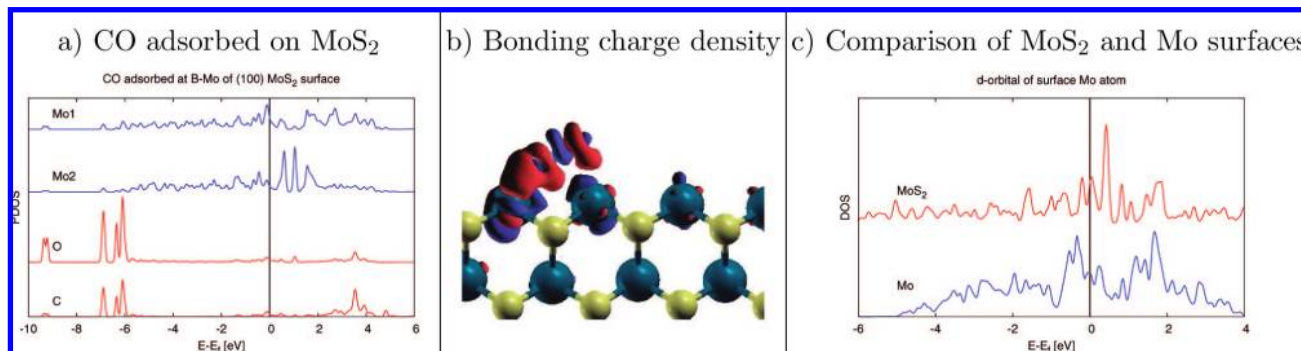


Figure 4. (a) Projected density of states of CO adsorbed at a bridge-Mo site of a MoS₂ surface. (b) Bonding charge density of CO adsorbed at a bridge-Mo. Red and blue colors represent positive and negative values, respectively. (c) Comparison of density of states of a surface Mo atom of a MoS₂ surface and Mo surface. The Fermi level is indicated by the vertical line at zero.

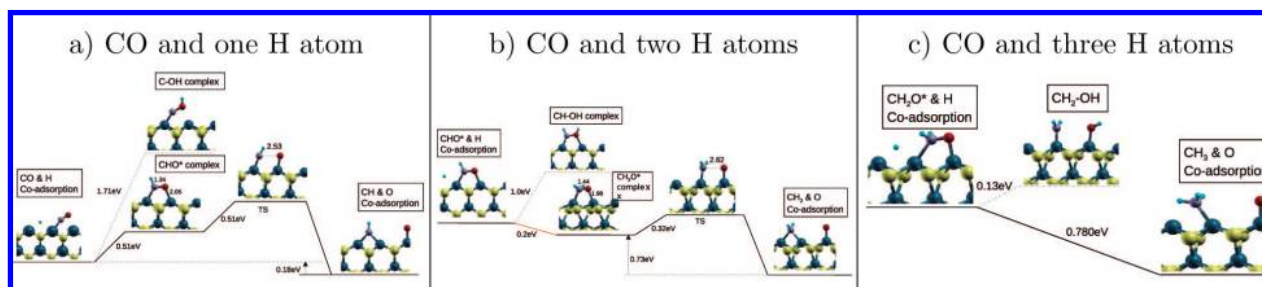


Figure 5. Energy diagram for sequential hydrogenation of CO by H atoms on a MoS₂ surface. Blue, yellow, gray, red, and light blue (small) spheres represent Mo, S, C, O, and H atoms, respectively. The unit for labeled C–O and Mo–O bond length is Å. (a) CO reacts with one H atom. (b) CO reacts with two H atoms. (c) CO reacts with three H atoms.

H on a Mo-edge of a MoS₂ surface was fairly mobile. Similar mobile hydrogen was also predicted on a Mo₂₇S₅₄ cluster.²⁸ The calculated activation energy for atomic H diffusion from a bridge-Mo site to a nearby symmetric equivalent bridge-Mo site on a Mo-edge of a MoS₂ surface is predicted to be ~ 0.20 eV. Hence, in the Fischer–Tropsch process for a MoS₂ surface from syngas, a H₂ molecule will supply atomic H.

C. Reaction of CO and H Atoms on a Mo-Edge of a MoS₂ Surface. Adsorbed CO was predicted to be unlikely to dissociate on a MoS₂ surface as described above, and the adsorbed CO molecules would react with the spontaneously dissociated hydrogen atoms in the Fischer–Tropsch reaction to yield products. This process is described in the following individual steps of CO hydrogenation.

1. CO and One H Atom. The coadsorption configuration is shown in Figure 5a with CO and a H atom located at nearby bridge-Mo sites. Because atomic H is mobile on the surface (calculated barrier energy is predicted as low as 0.20 eV), it is likely to be located at a metastable top-Mo site and react with adsorbed CO at a Mo bridge (adsorbed CO and H share one Mo atom) to form the CHO* complex spontaneously on the surface, which is 0.51 eV less stable than the coadsorption configuration. The formed CHO* complex is not a stable structure, as it will dissociate to a configuration with a CH* complex and atomic O coadsorbed on the surface, which is 0.18 eV more stable than the coadsorption configuration of CO and H (Figure 5a). The calculated activation energy is 0.51 eV. The transition state (TS) is with CH and O located at the titled top-Mo site (Figure 5a). Our frequency calculation results show that -541 cm⁻¹ was obtained for this TS configuration. It is noteworthy that the migration of a H atom results in a C–O bond parallel to a surface Mo–Mo bond and thus is highly activated, as indicated by the long C–O distance of 1.34 Å compared with the distance of 1.22 Å for the bridge site-adsorbed CO. The CO molecule in the CHO* complex tilted

more toward the surface, resulting in a Mo–O distance of 2.05 Å, which is close to the calculated Mo–O bond length of 2.03 Å for atomic O adsorbed on a surface. Therefore, for a covalent bond formed between an O atom and surface Mo atom, the C–O bond is predicted to be a weaker single bond rather than a double bond. It is not surprising that the dissociation of a CHO* complex is favored. We also found that a C–OH complex is ~ 1.20 eV less stable than a CHO* complex on a surface. Therefore, a CHO* complex and CH are relevant intermediates for the reaction of CO and one H atom.

2. CO and Two H Atoms. A CHO* complex is an intermediate species on a MoS₂ surface; it may capture one more H atom to form a more complicated complex. The coadsorption configuration is a CHO* complex described together with a H atom adsorbed at a nearby bridge-Mo site (Figure 5b). A slightly more stable configuration was found, namely, a CH₂O* complex on a surface (Figure 5b), which is different from that in the case of the one H atom. However, it is not surprising as the C atom in a CH₂O* complex is 4-fold coordinated. Meanwhile, a CH₂O* complex dissociates easier to a CH₂ complex and atomic O than does a CHO* complex. This is indicated by the larger energy difference between a CH₂O* complex and the coadsorption of a CH₂ complex and atomic O on a MoS₂ surface (0.73 eV), together with the smaller barrier energy of 0.32 eV. Similar to the cases of CO and CHO* complexes, the transition state is CH₂ and O adsorbed at the metastable top-Mo sites. Similar to the case of CHO*, our frequency calculation produced an imaginary value of -366 cm⁻¹ for the TS configuration. The C–O bond length in a CH₂O* complex is 0.11 Å longer than that of a CHO* complex, and CO is further tilted toward the surface, resulting in a Mo–O length being the same as that for adsorbed atomic O. We also found a CH–OH complex is ~ 1.20 eV less favored than a CH₂O* complex configuration, which is the same as in the case of one H atom. The main intermediates for continued CO hydrogenation are CH₂O* and CH₂.

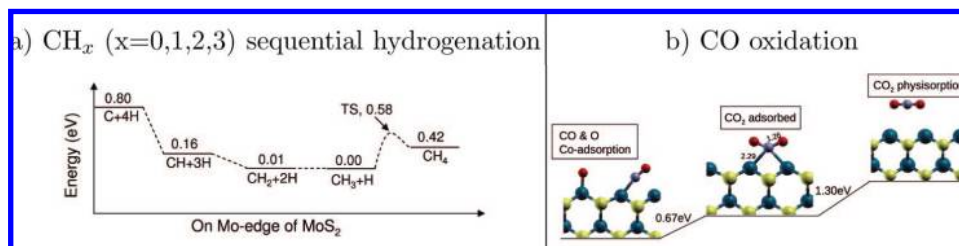


Figure 6. Thermodynamic energetic scheme of CH_x ($x = 0, 1, 2,$ and 3) sequential hydrogenation system and diagram for CO oxidation.

3. CO and Three H Atoms. When one more H atom was added to a CH_2O^* complex, the obtained structure is either a coadsorption of a CH_2O^* complex and a H atom adsorbed at a nearby bridge-Mo site or a spontaneous coadsorption of CH_3 and atomic O (Figure 5c). The latter structure is favored by 0.78 eV energy than the former. Because in a CH_2O^* complex the coordination of a C atom has already been saturated, it is not likely to form a CH_3O^* complex. A weak C–O bond in a CH_2O^* complex allows the C–O bond break easily and form a C–H bond when atomic H available. Furthermore, when an O atom in a CH_2O^* complex captures a H atom, an unstable configuration, which is 0.91 eV higher in energy, was obtained as the coadsorption of the CH_2 and OH species. This similar configuration was not predicted in the cases of the CO reactions with both one and two H atoms, further showing the cleavage of a C–O bond in a CH_2O^* complex is quite easy as indicated by the long C–O bond length and short Mo–O bond length. The dominant intermediate species is therefore CH_3 .

4. Desorption of CH_4 and CO_2 . Once a formed CH_3 intermediate species reacts further with a H atom, methane will form. A methane molecule was found to physisorb on a MoS_2 surface with a low adsorption energy of 0.16 eV. The desorption of methane from CH_3 and H on a MoS_2 surface is shown in Figure 6a. The calculated barrier energy is ~ 0.58 eV.

Adsorbed CO molecules react with oxygen atoms from the dissociation of the CHO^* and CH_2O^* species, resulting in CO_2 adsorbed on a surface spontaneously (when top-site O and CO share a Mo atom). The chemisorption energy is 1.60 eV and physisorption energy is 0.30 eV. The adsorbed CO_2 is a bent structure with a O–C–O bond angle of 134.5° . Although the coadsorption configuration of CO and atomic O is more energetically favored by 0.67 eV than that of CO_2 adsorbed on a MoS_2 surface, the adsorption of CO is strong with high adsorption energy showing that adsorbed CO molecules are very rich on a surface. The formation of CO_2 is becoming more likely. The calculated barrier energy of desorption of CO_2 is 1.30 eV, which is larger than the value of 1.0 eV for CO_2 desorption on a Au (110) surface³⁸ (Figure 6b).

IV. Discussion

According to Muramatsu et al.,³⁹ the dissociated CO favors chain propagation, leading to the synthesis of higher hydrocarbons and alcohols, whereas the nondissociated CO favors synthesis of the C_1 product. In contrast to the typical Fischer–Tropsch synthesis catalysts such as iron, which dissociate CO easily; our calculated results show that the MoS_2 catalyst does not dissociate CO. The most likely intermediate species of the CO hydrogenation reaction from syngas on a pure MoS_2 catalyst surface are CH_3 and O, which can be further converted to CH_4 and CO_2 by atomic H and CO on surfaces, respectively. These results are in agreement with the previous in situ diffuse reflectance infrared Fourier transform (DRIFT) study on sulfide $\text{Mo}/\gamma\text{-Al}_2\text{O}_3$ catalysts, which showed the main

products of CO hydrogenation are CH_4 and CO_2 .⁶ For the hydrogen-mediated CO dissociation, the CHO^* and CH_2O^* intermediate species are adsorbed on the surface, where the cleavage of the C–O bond (i.e., dissociation of CHO^* and CH_2O^* to CH and O or CH_2 , CH_3 , and O) is facilitated, with significantly low barrier energies more than 2.0 eV lower than that of direct C–O bond cleavage. These show the hydrogenation routine is the main reaction pathway rather than the carbide mechanism on a MoS_2 surface. Interestingly, many recent studies also indicated that CHO^* and CH_2O^* are important reaction intermediates in the Fischer–Tropsch process on metal surfaces.^{40–44} The difference between metal surfaces and a MoS_2 surface is that the reverse reactions of forming CH_xO are not favored on a MoS_2 surface.

We also studied the relative energies of adsorption of the possible intermediate species of OH and CH_x ($x = 1, 2,$ and 3) on a surface. The OH^* species adsorbed on a surface is 0.60 eV less favorable than coadsorption of atomic O and atomic H. Even in the more complicated structures, including the reaction of CO and H atoms, our calculations showed that the OH^* species is at least 0.91 eV less stable on a MoS_2 surface. Therefore, alcohols are difficult to form on a pure MoS_2 surface, and the intermediate species of O will be converted to CO_2 by a CO molecule, not H_2O . The CH_x ($x = 1, 2,$ and 3) species were found to chemisorb on a MoS_2 surface at a bridge-Mo site with adsorption energies of 6.48, 4.55, and 2.62 eV, respectively (Table 2). The sequential hydrogenation of CH_x ($x = 0, 1, 2,$ and 3) on MoS_2 is exothermic, as shown in Figure 6a, except for the desorption of CH_4 , which physisorbs on a MoS_2 surface, in contrast to the cases of CH_x ($x = 1, 2,$ and 3). These confirm that the main products of CO hydrogenation on a MoS_2 surface are CO_2 and CH_4 . However, the early experimental study showed that pure MoS_2 yielded hydrocarbons composed mostly of linear alkanes,⁴ which is different from our results. Alkyl chain growth was also investigated. Because dissociation of CO is difficult, the possible prototypical CH_x coupling reactions are CH–CH, CH– CH_2 , CH– CH_3 , CH_2 – CH_2 , CH_2 – CH_3 , and CH_3 – CH_3 . Our calculations showed that all of the CH_x coupling reactions are energy unfavored by up to 0.64 eV. The study of CH_3 – CH_3 coupling shows the methane is unlikely to be formed, not only because of the higher energy of methane on MoS_2 but also because of the saturated coordination of C in CH_3 . The barrier energy for formation of C_2H_6 is therefore predicted to be high. This again shows CH_4 is the main CO hydrogenation product on a pure MoS_2 surface.⁶ Doped with alkali and other promoters, the formate species for reaction from syngas on a MoS_2 catalyst is converted to methanol and higher alcohols and hydrocarbons. Hence, the effects of promoters and chain growth will be future research topics.

V. Conclusions

We have performed a systematic density functional theory study on the hydrogenation reaction of syngas on a pure MoS₂ surface. CO was found to adsorb at a bridge-Mo site with a tilted configuration and a longer C–O bond length than that of free CO. We also found the dissociation of CO was difficult on a MoS₂ surface, which is different from the typical heterogeneous catalysts used in a Fischer–Tropsch synthesis such as iron and a Mo metal surface that dissociate CO easily. The calculated barrier energy is as high as 2.60 eV. Different dissociation properties of CO on MoS₂ and Mo surfaces resulted from the different structural properties of CO adsorbed on surfaces and different catalyst activity of MoS₂ and a Mo surface. The H₂ molecule was found to dissociate spontaneously on a MoS₂ surface, which will supply H atoms in the hydrogenation reaction. Our calculation also showed the hydrogenation routine is the main reaction pathway on a MoS₂ surface.

The calculation showed the most likely products of CO hydrogenation on a MoS₂ surface are CH₄ and CO₂, which is in agreement with experiment results.⁶ The hydrogenation of CH_x on a MoS₂ surface is exothermic, showing the formation of methane on the surface. Further study of alkyl chain growth and adsorption of intermediate species of OH* on a MoS₂ surface confirms the result. However, addition of promoters such as potassium, nickel, or cobalt on a MoS₂ surface causes the products of a hydrogenation reaction from syngas to convert to alcohols or higher hydrocarbons. The effect of promoters will be our next research topic.

Acknowledgment. This research is supported by Nanostellar. We thank Dr. Bin Shan for helpful discussions. Calculations were done by the Texas Advanced Computing Center (TACC). Graphics have been generated with the XCRYSDEN computer program.⁴⁵

References and Notes

- (1) Donath, E. E. In *Catalysis: Science and Technology*; Anderson, J. R., Boudart, M., Eds.; Springer: Berlin, 1982.
- (2) Song, C. *Catal. Today* **2003**, *86*, 211.
- (3) Fukase, S.; Akashah, S. *Technology, Catalyst Supplement Part 1. Hydrocarbon Asia*, March/April, 2004, 24.
- (4) Lee, J. S.; Kim, S.; Lee, K. H.; Nam, I.; Chung, J. S.; Kim, Y. G.; Woo, H. C. *Appl. Catal., A* **1994**, *110*, 11.
- (5) Zhang, J.; Wang, Y.; Chang, L. *Appl. Catal., A* **1995**, *126*, L205.
- (6) Koizumi, N.; Bian, G.; Murai, K.; Ozaki, T.; Yamada, M. *J. Mol. Catal. A: Chem.* **2004**, *207*, 173.
- (7) Murchison, C. B.; Conway, M. M.; Stevens, R. R.; Quarder, G. In *Proceedings of the Ninth International Congress on Catalysis*; Phillips, M. J., Ternan, M., Eds.; Chemical Institute of Canada: Ottawa, Canada, 1988; Vol. 2, p 626.
- (8) Li, Z.; Fu, Y.; Bao, J.; Jiang, M.; Hu, T.; Liu, T.; Xie, Y. *Appl. Catal., A* **2001**, *220*, 21.
- (9) Iranmahboob, J.; Hill, D. O. *Catal. Lett.* **2002**, *78*, 49.
- (10) Iranmahboob, J.; Toghiani, H.; Hill, D. O. *Appl. Catal., A* **2003**, *247*, 207.

- (11) Li, D.; Yang, C.; Qi, H.; Zhang, H.; Li, W.; Sun, Y.; Zhong, B. *Catal. Commun.* **2004**, *5*, 605.
- (12) Li, D.; Yang, C.; Li, W.; Sun, Y.; Zhong, B. *Top. Catal.* **2005**, *32*, 233.
- (13) Steynberg, A. P.; Dry, M., Eds. *Studies in Surface Science and Catalysis*; Elsevier: Amsterdam, 2004, Vol. 152.
- (14) Bartosch, C. E.; Whitman, L. J.; Ho, W. *J. Chem. Phys.* **1986**, *85*, 1052.
- (15) Sorescu, D. C.; Thompson, D. L.; Hurley, M. M.; Chabalowski, C. F. *Phys. Rev. B* **2002**, *66*, 035416.
- (16) Curulla-Ferre, D.; Govender, A.; Bromfield, T. C.; Niemantsverdriet, J. W. *J. Phys. Chem. B* **2006**, *110*, 13897.
- (17) Zaera, F.; Kollin, E.; Gland, J. L. *Chem. Phys. Lett.* **1985**, *121*, 464.
- (18) Fulmer, J. P.; Zaera, F.; Tysoe, W. T. *J. Chem. Phys.* **1987**, *87*, 7265.
- (19) Colaianni, M. L.; Chen, J. G.; Weinberg, W. H.; Yates, J. T., Jr. *J. Am. Chem. Soc.* **1992**, *114*, 3735.
- (20) Ji, Z.; Li, J.-Q. *J. Phys. Chem. B* **2006**, *110*, 18363.
- (21) Scheijen, F. J. E.; Niemantsverdriet, J. W.; Ferre, D. C. *J. Phys. Chem. C* **2007**, *111*, 13473.
- (22) Iranmahboob, J.; Gardner, S. D.; Toghiani, H.; Hill, D. O. *J. Colloid Interface Sci.* **2004**, *270*, 123.
- (23) Muller, B.; van Langeveld, A. D.; Moulijn, J. A.; Knozinger, H. *J. Phys. Chem.* **1993**, *97*, 9028.
- (24) Elst, L. P. A. F.; Eijssbouts, S.; van Langeveld, A. D.; Moulijn, J. A. *J. Catal.* **2000**, *196*, 95.
- (25) Peri, J. B. *J. Phys. Chem.* **1982**, *86*, 1615.
- (26) Zeng, T.; Wen, X.; Wu, G.; Li, Y.; Jiao, H. *J. Phys. Chem. B* **2005**, *109*, 2846.
- (27) Cristol, S.; Paul, J. F.; Payen, E.; Dougeard, D.; Clemendot, S.; Hutschka, F. *J. Phys. Chem. B* **2002**, *106*, 5659.
- (28) Wen, X.; Zeng, T.; Teng, B.; Zhang, F.; Li, Y.; Wang, J.; Jiao, H. *J. Mol. Catal. A* **2006**, *249*, 191.
- (29) Baroni, S.; Dal Corso, A.; de Gironcoli, S.; Giannozzi, P. *Plane-Wave Self-Consistent Field*. <http://www.pwscf.org>.
- (30) Perdew, J. P.; Wang, Y. *Phys. Rev. B* **1992**, *45*, 13244.
- (31) Vanderbilt, D. *Phys. Rev. B* **1990**, *41*, 7892.
- (32) Monkhorst, H. J.; Pack, J. D. *Phys. Rev. B* **1976**, *13*, 5188.
- (33) Jonsson, H.; Mills, G.; Jacobsen, K. W. *Classical and Quantum Dynamics in Condensed Phase Simulations*; World Scientific: Singapore, 1998.
- (34) Helveg, S.; Lauritsen, J. V.; Laegsgaard, E.; Stensgaard, I.; Norskov, J. K.; Clausen, B. S.; Topsoe, H.; Besenbacher, F. *Phys. Rev. Lett.* **2000**, *84*, 951.
- (35) Lauritsen, J. V.; Kibsgaard, J.; Helveg, S.; Topsoe, H.; Clausen, B. S.; Laegsgaard, E.; Besenbacher, F. *Nat. Nanotechnol.* **2007**, *2*, 53.
- (36) Chackerian, C., Jr. *J. Chem. Phys.* **1976**, *65*, 4228.
- (37) Bliggard, T.; Norskov, J. K.; Dahl, S.; Matthiesen, J.; Christensen, C. H.; Sehested, J. *J. Catal.* **2004**, *224*, 206.
- (38) Gottfried, J. M.; Christmann, K. *Surf. Sci.* **2004**, *566–568*, 1112.
- (39) Muramatsu, A.; Tatsumi, T.; Tominaga, H. *J. Phys. Chem.* **1992**, *96*, 1334.
- (40) Wang, S.; Cao, D.; Li, Y.; Wang, J.; Jiao, H. *J. Phys. Chem. B* **2006**, *110*, 9976.
- (41) Huo, C.; Ren, J.; Li, Y.; Wang, J.; Jiao, H. *J. Catal.* **2007**, *249*, 174.
- (42) Inderwildi, O. R.; Jenkins, S. J.; King, D. A. *J. Phys. Chem. C* **2008**, *112*, 1305.
- (43) Huo, C.; Li, Y.; Wang, J.; Jiao, H. *J. Phys. Chem. C* **2008**, *112*, 14108.
- (44) Inderwildi, O. R.; Jenkins, S. J.; King, D. A. *Angew. Chem., Int. Ed.* **2008**, *47*, 5253.
- (45) Kokalj, A. *J. Mol. Graphics Modell.* **1999**, *17*, 176, code available from <http://www.xcrysden.org>.

JP807705Y